Improved variational calculations of nucleon matter

J. Morales, Jr., V. R. Pandharipande, and D. G. Ravenhall
Department of Physics, University of Illinois at Urbana-Champaign, 1110 West Green Street, Urbana, Illinois 61801
(Received 14 June 2002; published 27 November 2002)

Variational calculations of nucleon matter, either symmetric nuclear or pure neutron matter, use Fermi hypernetted chain and single-operator chain summation methods to sum approximately the contributions of clusters of $\geqslant 3$ nucleons to the energy expectation value. The cluster contributions summed by these methods are discussed in detail, and it is shown that for realistic interactions the 3-body cluster contribution is larger than the sum of $\geqslant 4$-body contributions. We present a new method, based on representing cluster wave functions by multidimensional vectors in spin-isospin space, as is common in quantum Monte Carlo calculations of light nuclei, to calculate exactly the 3-body cluster contribution including 3-body forces and all but spin-orbit correlations. The variational energies obtained with the Argonne $v18$ 2- and Urbana IX 3-nucleon interactions, using the exact 2- and 3-body cluster contributions and the approximate $\geqslant 4$-body contributions summed with chain summation techniques are lower, closer to the empirical values for symmetric nuclear matter than in previous calculations using the operator chain summation approximation for the large 3-body cluster. In pure neutron matter the operator chain summation approximation is found to be fairly accurate for the 3-body cluster; the present results are only slightly higher than the previous ones. We also report on the results for the Argonne $v14$ 2-nucleon interaction without any 3-body interaction. This case has been studied with Brueckner's method including 2, 3, and parts of 4-hole line terms by Day and Wiringa [Phys. Rev. C **32**, 1057 (1985)]. Our results are significantly lower than theirs.

DOI: 10.1103/PhysRevC.66.054308 PACS number(s): 21.65.+f, 26.60.+c

I. INTRODUCTION

In the past few years it has been shown that the energies of all the bound states of up to ten nucleons can be well reproduced by essentially exact Green's function Monte Carlo (GFMC) calculations with realistic models of 2- and 3-nucleon interactions [1–4]. The error in these calculations is estimated to be less than 2% of the calculated energy. The computational effort in the GFMC calculations increases exponentially with the number of nucleons; and with the present computing resources ^{12}C may be the largest symmetric nucleus that can be studied with this method.

The uniform nucleon matter problem has been studied with realistic nuclear forces since the pioneering work of Brueckner, Bethe, and Goldsone in the 1950s as a step towards a microscopic theory of large nuclei, and more recently for studying the structure of neutron stars and supernovas [5,6]. GFMC calculations of symmetric nuclear matter (SNM) with equal number of neutrons and protons are not yet possible. However, Carlson has recently calculated energies for 14 neutrons in a periodic box with semirealistic interactions [7] with the GFMC method, and attempts to extract the $E(\rho)$ of pure neutron matter (PNM) from these results are in progress. A new quantum Monte Carlo method using auxiliary fields is also being developed by Schmidt and Fantoni [8] with which it may be possible to address the nucleon matter problem. At present, it is being used to study PNM [9].

All available calculations of SNM with realistic interactions use methods based on cluster expansions. In the Brueckner approach a hole line expansion is made for $H_I = H - T - U$, where H is the full Hamiltonian, T is the kinetic energy operator, U is a single-particle potential to be chosen, and $H_0 = T + U$. 2- and 3-hole line terms of this expansion are calculated with 2-body forces [10] for two different choices of U, and in his pioneering calculations Day also estimated parts of 4-hole line terms [11]. In this approach one attempts to choose U to improve convergence of the expansion; however, higher-order terms are difficult to calculate. In most available calculations the 3-nucleon interaction is approximated with a density dependent 2-nucleon interaction [12].

The variational method is conceptually much simpler and 3-nucleon interactions can be easily included in the Hamiltonian. However, with plausible variational wave functions the cluster expansion of the energy expectation value does not converge rapidly. In most calculations with realistic interactions [13–15], the leading contributions of all clusters are summed by Fermi-hypernetted chain (FHNC) and single-operator chain (SOC) integral equations. For brevity we call this the chain summation method (CSM). In this method only the 2-body cluster contribution is exact, and all $n \geqslant 3$ body cluster contributions are approximated, but the series is not truncated.

In principle, variational calculations provide an upper bound to the ground state energy. The bound is closer to the true energy when the variational wave function can well reproduce the exact eigenfunction. In practice a correction to the variational energy is estimated to take into account the limitations of the variational wave function using either correlated basis theory [16,17] or simpler methods [14].

In this paper we describe a new matrix method to calculate the 3-body cluster contribution exactly for static correlations including 3-nucleon interactions. The small 3-body cluster contributions from momentum dependent spin-orbit correlations are omitted from this exact calculation; they are estimated approximately. This method provides a test for the accuracy of the SOC approximation in CSM; the FHNC is

exact for $n=3$. We also present results for SNM and PNM using exact computations of 2- and 3-body clusters, and CSM approximation for the rest. The method is useful for Hamiltonians in which the part evaluated with the CSM approximation is relatively small.

The cluster expansion of nucleon matter energy is briefly described in Sec. II where we present CSM estimates of (2–5)-body cluster contributions for the Argonne $v18$ 2-nucleon [18] and Urbana IX 3-nucleon interaction [19]. The matrix method to calculate the 3-body cluster contribution is described in Sec. III, and the results are presented in Sec. IV. In earlier calculations of Akmal and Pandharipande (AP) [14] with these interactions and the CSM, the energy of SNM at the empirical equilibrium density of $\rho_0 = 0.16$ fm^{-3} was estimated to be -12 MeV, about 25% higher than the empirical value of -16. With the present method we obtain ~ -14 MeV. The AP, as well as present estimates, include a perturbative correction of ~ -2 MeV to take into account the limitations of the variational wave function [14]. The calculated equilibrium density is close to ρ_0 in both the CSM and present calculations.

The CSM estimate of the 3-body cluster energy in PNM is found to be fairly accurate for this Hamiltonian. The present PNM results are only slightly above those of AP.

We also report on the results for SNM with the older Argonne $v14$ interaction which has been used in many Brueckner and variational calculations. At $k_F=1.6$ fm^{-1} the present method gives $E\sim -22.3$ MeV, lower than Day's estimate of -17.8 ± 1.3 MeV. However, the CSM is found to be less accurate for this Hamiltonian.

The combination of $v18+U$-IX interactions used here underbinds $N\sim Z$ light nuclei like ^{7}Li and ^{8}Be by $<4\%$ in GFMC calculations with an error $<2\%$. The more accurate Illinois models of 3-nucleon interaction reproduce the experimental energies of light nuclei within the GFMC accuracy. However, these models contain 3-pion exchange interactions that have very complex spin-isospin dependence [2]. The present method has been developed partly to perform nucleon matter calculations with the Illinois models of V_{ijk}, which are in progress. Conclusions and outlook for more accurate calculations of nucleon matter are given in Sec. V.

II. CLUSTER EXPANSION OF NUCLEON MATTER ENERGY

The Hamiltonian containing the Argonne $v18$ 2-nucleon and the Urbana IX 3-nucleon interaction is discussed in detail by AP. The $v18$ interaction has 14 isoscalar terms given by

$$v_{ij}=\sum_{p=1,14} v_p(r_{ij})O_{ij}^p. \tag{2.1}$$

The pair operators with odd values of p are

$$O_{ij}^{p=odd}=1,\ \boldsymbol{\sigma}_i\cdot\boldsymbol{\sigma}_j,\ S_{ij},\ \mathbf{L}\cdot\mathbf{S},\ L^2,\ L^2\boldsymbol{\sigma}_i\cdot\boldsymbol{\sigma}_j,\ (\mathbf{L}\cdot\mathbf{S})^2. \tag{2.2}$$

Here S_{ij} and $\mathbf{L}\cdot\mathbf{S}$ are the tensor and spin-orbit operators. The operators with even values of p are

$$O_{ij}^{p=even}=O_{ij}^{p-1}\boldsymbol{\tau}_i\cdot\boldsymbol{\tau}_j. \tag{2.3}$$

The remaining four operators in the $v18$ interaction break the isopin symmetry. They do not contribute to the energy of SNM in first order, and are included in PNM calculations as described in Ref. [14].

It is convenient to define the Hamiltonian as

$$H=T_F+(T-T_F)+\sum_{i<j}(v_{ij}^s+v_{ij}^b+v_{ij}^q)+\sum_{i<j<k}V_{ijk}, \tag{2.4}$$

where $T_F=0.3k_F^2/m$ is the Fermi-gas kinetic energy. The 2-nucleon interaction is divided into its static part v_{ij}^s containing terms with momentum independent operators $O_{ij}^{p=1,6}$, the spin-orbit part v_{ij}^b with $O_{ij}^{p=7,8}$, and the quadratic part v_{ij}^q including terms having $O_{ij}^{p=9,14}$. Different approximations are used to calculate the expectation values of these three parts of v_{ij}. The Urbana-IX V_{ijk} is static and is treated along with the v_{ij}^s.

The variational wave function used in the above mentioned calculations of nucleon matter is of the form

$$|\Psi_V\rangle=\left[\mathcal{S}\prod_{i<j}F_{ij}\right]|\Phi_A(k_F)\rangle, \tag{2.5}$$

where F_{ij} are the pair correlation operators,

$$F_{ij}=\sum_{p=1,8}f_p(r_{ij})O_{ij}^p, \tag{2.6}$$

and $|\Phi_A(k_F)\rangle$ is the antisymmetric Fermi-gas wave function. The F_{ij} do not commute with F_{ik}, hence it is necessary to symmetrize their product. By convention, the spatial correlation $f_{p=1}(r_{ij})$ is denoted by $f_c(r_{ij})$, and all the other correlations, $p\neq c$, have spin-isospin dependence. We divide the F_{ij} into its static ($p=1,6$) and spin-orbit ($p=7,8$) parts:

$$F_{ij}=F_{ij}^s+F_{ij}^b\ ; \tag{2.7}$$

they are treated separately.

The cluster expansion for the energy

$$E=T_F+\frac{\left\langle\Phi_A(k_F)\left|\left[\mathcal{S}\prod_{i<j}F_{ij}\right](H-T_F)\left[\mathcal{S}\prod_{i<j}F_{ij}\right]\right|\Phi_P(k_F)\right\rangle}{\left\langle\Phi_A(k_F)\left|\left[\mathcal{S}\prod_{i<j}F_{ij}\right]\left[\mathcal{S}\prod_{i<j}F_{ij}\right]\right|\Phi_P(k_F)\right\rangle} \tag{2.8}$$

is obtained by replacing F_{ij} by $[(F_{ij}-1)+1]$ and expanding in powers of $(F_{ij}-1)$. The bra $\langle\Phi_A(k_F)|$ is antisymmetric, while the ket $|\Phi_P(k_F)\rangle$ is a simple product of single-particle states in which nucleons $i,j,\ldots$ occupy plane wave states with momenta $\mathbf{k}_i,\mathbf{k}_j,\ldots,$ and spin-isospin $\chi_i,\chi_j,\ldots$. The cluster expansion for the energy of nucleon matter [20] is complicated by the presence of noncommuting spin-isospin

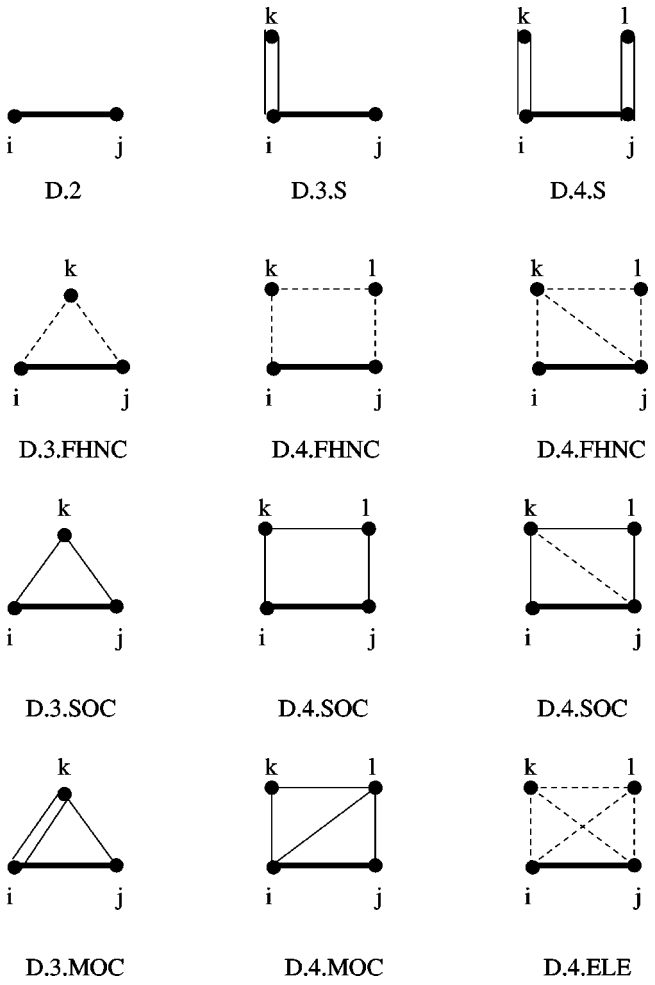

FIG. 1. Examples of direct diagrams illustrating various cluster contributions to the energy of nucleon matter.

correlations and interactions. The additional presence of momentum dependent terms in the H and F makes it even more complex [21,14].

The simplest expansion is of the expectation values of the static potentials v_{ij}^s and V_{ijk} including only the static F^s. The spin-orbit correlations have gradient operators, therefore their contribution is more complex [21]. For brevity, we review here only the cluster expansion for the expectation value of v_{ij}^s, with F^s correlations to introduce the notation and orient the readers. It contains connected diagrams formed with finite range correlation bonds $(f_c^2(r_{ij})-1)$, $2f_c(r_{ij})f_p(r_{ij})$, and $f_p(r_{ij})f_q(r_{ij})$, with indices p and $q \neq c$, and the spatial exchange correlation represented by the Slater function $l(r_{ij})$:

$$l(r)=\frac{n_{\sigma\tau}}{\rho}\sum_{\mathbf{k}<k_F} e^{i\mathbf{k}\cdot\mathbf{r}}=3[\sin(x)-x\cos(x)]/x^3. \quad (2.9)$$

Here $x=k_F r$, ρ is the matter density, and $n_{\sigma\tau}=4$ and 2 is the spin-isospin degeneracy of SNM and PNM, respectively.

For example, some of the direct cluster diagrams that contribute to the expectation value of v_{ij}^s are shown in Fig. 1. The dots in these diagrams show nucleon positions $\mathbf{r}_i, \mathbf{r}_j, \ldots,$ and the thick line represents $f_p(r_{ij})v_q(r_{ij})f_r(r_{ij})$ with $p,q,r \leqslant 6$. The contribution of the 2-body direct diagram $D.2$ of Fig. 1 to the energy of SNM is given by

$$[v_{ij}^s-2b-\mathrm{dir}]=\frac{\rho}{2}\sum_{p,q,r=1,6} C[O_{ij}^p O_{ij}^q O_{ij}^r] \times \int d^3r_{ij}\ \ f_p(r_{ij})v_q(r_{ij})f_r(r_{ij}). \quad (2.10)$$

Here $C[O_{ij}^p O_{ij}^q O_{ij}^r]$ is the spin-isospin independent part, called the C-part [20], of the product of operators. Other parts of the operator product are linear in spins or isospins, and they do not contribute to the direct 2-body cluster in SNM.

The 3-body direct cluster contribution to the expectation value of v_{ij}^s with the static F^s correlation operator is given [20] by

$$[v_{ij}^s-3b-\mathrm{dir}]=\frac{\rho^2}{2}\frac{1}{n_{\sigma\tau}^3}\sum_{\chi_i,\chi_j,\chi_k}\int d^3r_{ij}d^3r_{ik}\langle\chi_i^\dagger,\chi_j^\dagger,\chi_j^\dagger| \times(\mathcal{M}v_{ij}^s\mathcal{M}-F_{ij}^s v_{ij}^s F_{ij}^s(F_{jk}^{s2}+F_{ki}^{s2}-1)) \times|\chi_i,\chi_j,\chi_k\rangle, \quad (2.11)$$

where $\mathcal{M}$ is the 3-body correlation operator

$$\mathcal{M}=[\mathcal{S}F_{ij}^s F_{jk}^s F_{ki}^s]. \quad (2.12)$$

In addition to the symmetrized product of pair operators, $\mathcal{M}$ can contain explicit 3-body operators [22] neglected here and in variational wave function [Eq. (2.5)]. This contribution [Eq. (2.11)] contains a sum over the possible spin-isospin states $\chi=n\uparrow$ and $n\downarrow$ in PNM and $n\uparrow$, $n\downarrow$, $p\uparrow$ and $p\downarrow$ in SNM. The densities of each spin-isospin species are $\rho/n_{\sigma\tau}$, and the factor $1/n_{\sigma\tau}^3$ in the $[v_{ij}^s-3b-\mathrm{dir}]$ takes that into account. It includes the term

$$\mathcal{M}\ \ v_{ij}^s\mathcal{M}-F_{ij}^s v_{ij}^s F_{ij}^s \quad (2.13)$$

from the expansion of the numerator of the expectation value [Eq. (2.8)], and the term

$$-F_{ij}^s v_{ij}^s F_{ij}^s(F_{jk}^{s2}+F_{ki}^{s2}-2), \quad (2.14)$$

in which the factor $(F_{jk}^{s2}+F_{ki}^{s2}-2)$ comes from the expansion of the denominator.

When the F^s operators are approximated by $f_c(r)$, the spin-isospin sum gives a factor $n_{\sigma\tau}^3$ to cancel the $1/n_{\sigma\tau}^3$, and we can commute the f_c's in the $\mathcal{M}\ v_{ij}^s\ \mathcal{M}$ to form f_c^2. The second term then cancels the separable parts, i.e., those that have only jk or ki correlation bonds, of the first, and we obtain the well-known irreducible contribution:

$$[v_{ij}^s - 3b - dir - \text{Jastrow}] = \frac{\rho^2}{2}\int d^3r_{ij}d^3r_{ik} f_c^2(r_{ij}) v_{ij}^s \times (f_c^2(r_{jk})-1)(f_c^2(r_{ki})-1), \tag{2.15}$$

appropriate for the Jastrow variational wave function, $F = f_c$. This contribution is included in the diagram D.3.FHNC in Fig. 1. The dashed lines in this diagram denote $f_c^2(r)-1$. It is contained in the FHNC [23] sum together with all of its exchange terms without approximation.

In the SOC approximation the F_{ij}^s multiplying the v_{ij}^s are not approximated, but only the leading terms with two spin-isospin correlations of the spectator nucleon k, having either $f_p(r_{jk})f_q(r_{ki})$ or $f_p(r_{jk})f_q(r_{jk})$ or $f_p(r_{ki})f_q(r_{ki})$ are calculated. These terms are denoted by diagrams D.3.SOC and D.3.S in Fig. 1. In direct diagrams, terms with a single spin-isospin correlation of k give zero contribution after summing over the spin-isospin states of nucleon k. A single thin line, as in diagram D.3.SOC, denotes $2f_{p\neq c}f_c$, while a double thin line, as in diagram D.3.S, denotes $f_{p\neq c}f_{q\neq c}$.

In the SOC approximation the contribution of 3-body terms with $f_p(r_{ki})f_q(r_{ki})$ are calculated exactly only in the limit where jk correlations are neglected. In this limit the contribution of D.3.S is given by [20]:

$$[v_{ij}^s - 3b.S - \text{dir}] = \rho^2 \sum_{p,q,r,s,t=1,6}\int d^3r_{ij} f_p(r_{ij}) v_q(r_{ij}) f_r(r_{ij}) \int d^3r_{ik} f_s(r_{ik}) f_t(r_{ik}) \times C[\tfrac{1}{4}\{O_{ij}^p, O_{ik}^s\} O_{ij}^q \{O_{ij}^r, O_{ik}^t\} - O_{ij}^p O_{ij}^q O_{ij}^r O_{ik}^s O_{ik}^t]. \tag{2.16}$$

At least one of the O_{ij} must not commute with the O_{ik} operators for this contribution to be nonzero. The contribution of the operator chain diagram D.3.SOC is given by [20]

$$[v_{ij}^s - 3b.\text{SOC} - \text{dir}] = \frac{\rho^2}{2}\sum_{p,q,r=1,6}\sum_{s,t\neq c}\int d^3r_{ij}d^3r_{ik} \times f_p(r_{ij}) v_q(r_{ij}) f_r(r_{ij}) \times [2f_c(r_{ik})f_s(r_{ik})] \times [2f_c(r_{jk})f_t(r_{jk})] \times C[\tfrac{1}{4}\{O_{ij}^p, O_{ik}^s\} O_{ij}^q \{O_{ij}^r, O_{jk}^t\}]. \tag{2.17}$$

Using the FHNC summation technique [23] it is possible to sum many-body diagrams with $[f_c^2(r)-1]$ correlations, such as those denoted by D.4.FHNC in Fig. 1. The diagrams summed by FHNC equations can have hypernetted chains. However, these equations do not sum elementary diagrams such as D.4.ELE in Fig. 1, having coupling between two or more chains of correlations. For Jastrow correlations, diagrams with a coupling between two hypernetted chains can be summed by the FHNC/4 equations [24]; they are smaller than those included in the FHNC. In contrast, the SOC equations [20] sum only the single-operator chain or ring diagrams such as D.4.S, D.4.SOC in Fig. 1. The C parts of the operator products are particularly simple to calculate for these diagrams. However, the multiple-operator chain (MOC) diagrams such as D.3.MOC and D.4.MOC are not included in SOC sums. See Ref. [20] for a more complete description of direct and exchange terms summed by the FHNC/SOC approximation denoted here by CSM.

The SOC approximation is valid when the spin-isospin correlations $f_{p\neq c}$ are much less than 1. Nevertheless, such correlations can give substantial many-body contributions due to their long range. For example, the contribution of D.4.SOC can be comparable to that of D.3.SOC when

$$\rho\int d^3r_l [2f_c(r_{lk})f_t(r_{lk})][2f_c(r_{jl})f_t(r_{jl})] \sim f_t(r_{jk}), \tag{2.18}$$

due to large ρ and/or the long range of the spin-isospin correlations. Some of the 3-body terms omitted in the SOC approximation have been estimated by Wiringa [25] and shown to be smaller than those summed by SOC equations. Here we propose to sum them all exactly, as discussed in Sec. III.

The complete 3-body cluster can have of order 50 different links on each side of the triangle formed by $\mathbf{r}_{ij}, \mathbf{r}_{jk}$, and $\mathbf{r}_{ki}$, producing of the order of 100 000 diagrams. Clusters with more than 3 bodies have an even larger number of terms. With the CSM [20,13,14] it is simpler to calculate the sums of all the diagrams included in that approximation than to separately sum the diagrams with a given number of particles or spin-isospin correlation bonds. Therefore the individual cluster contributions to the variational energy of nucleon matter were not calculated in previous studies. Nevertheless, they contain useful information.

The contributions to the expectation values from n-particle clusters with a specific number of spin-isopsin correlations can be easily obtained from the total. When k_F and ρ are treated as independent variables, the contribution of an n-particle cluster to the matter energy per nucleon is proportional to $\rho^{(n-1)}$. We calculate the total energy with ρ replaced by $x\rho$ for several values of x from 0 to 1. We also calculate it replacing $f_{p\neq c}(r)$ by $yf_{p\neq c}(r)$ for several values of y over the same interval. The calculated expectation value $Z(x,y)$ of any operator can be expanded in a polynomial of x and y whose coefficients contain the required information.

The Slater function $l(r)$ and the interaction operators are kept fixed, while varying x and y. In the present work we calculate the $E(x)$ at $y=1$ to study the cluster expansion of the energy expectation value.

In variational calculations the correlation functions $f_p(r)$ are obtained from 2-body Schrödinger-like equations with healing distances d_t for tensor correlations and d_c for all others. The spin-isospin dependent parts of the 2-nucleon interaction are quenched in the f equations by a parameter α. The variational parameters d_c, d_t, and α are determined by minimizing the energy with constraints imposing conservation of the number of nucleons and charge [13,14]. The correlation functions naturally depend upon the density, the neutron fraction of matter, and the assumed 2- and 3-nucleon interactions. Therefore the convergence of the cluster expansion also depends upon all these variables. In Tables I–VI we report on the cluster expansion of the energy of SNM and PNM at densities of $0.5\rho_0$, 1 and $1.5\rho_0$ for Hamiltonian containing the $v18$ and U-IX interactions. The $E(x)$ is calculated using the CSM used by AP. Minor improvements in the CSM are described later. Only the 2-body cluster contributions listed in these tables are exact; the values reported for $n\geqslant 3$ are sums of those n-body diagrams that are included in CSM. Tables VII and IX give results for PNM at $2\rho_0$, where AP find evidence for a phase transition.

The CSM variational energy and parameters are given in the table captions. The columns of the tables give contributions of clusters with 2–5 nucleons, the sum of all clusters with more than 5 nucleons, and the sum of all clusters. The row labeled v_{ij}^s lists contributions of v^s with only static F^s. These large contributions are obtained by summing all direct and exchange FHNC and SOC diagrams. Similarly, the T_s gives the contribution of only F^s correlations to $(T-T_F)$. All terms with either F^b and/or v^b are included in the row $v_{ij}^b+T_b$. They include the expectation value of v^b, which occurs mostly via F^b correlations, and the changes in the static interaction and kinetic energies due to F^b correlations. A restricted set of diagrams is included in the calculation of the effect of $L\cdot S$ correlations on kinetic and potential energies, due to the gradient operator in F^b. Both T_s and T_b are calculated with the Pandharipande-Bethe [26] expression for the kinetic energy.

The rows v_{ij}^q and V_{ijk}, respectively, give the contributions of these terms in the Hamiltonian. The 3-body contribution to v_{ij}^q is comparable to that of 2-body clusters. This is on account of new terms in the 3-body cluster in which the ∇_i^2 in v_{ij}^q operate on F_{ik}. In the earlier calculations of AP and APR (Ref. [15]), only the leading terms of the 3-body cluster contribution to v_{ij}^q were calculated. In the present work we have dressed this contribution with $\exp[G_{dd}(r_{ij})G_{dd}(r_{jk})G_{dd}(r_{ki})]$, where $G_{dd}(r_{ij})$ represent central direct-direct FHNC sums [20]. But, as can be seen from the tables, these do not give large >3-body cluster contributions to the v_{ij}^q expectation value. The contribution of F^b correlations to $n\geqslant 3$ clusters of v^q is neglected. There are also new 4-body terms in the expectation value of v_{ij}^q having $\nabla_i F_{ik}$ and $\nabla_i F_{il}$. They are expected to be small, and have not yet been estimated.

TABLE I. Cluster contributions calculated with CSM: SNM at $\rho=0.5\rho_0$, $\alpha=0.60$, $d_c=2.23$ fm and $d_t=8.93$ fm; $T_F=13.9$ MeV and $E_v^{CSM}=-7.1$ MeV.

n	2	3	4	5	>5	Total
v_{ij}^s	−36.5	7.4	−4.9	2.6	−0.9	−32.3
T_s	10.0	−1.6	1.4	−0.7	0.1	9.2
v_{ij}^q	1.2	0.8	0.0	0.0	0.0	1.9
V_{ijk}		0.6	0.1	0.1	0.0	0.7
$v_{ij}^b+T_b$	−0.6	0	0	0	0	−0.6
$E_v^{CSM}-T_F$	−25.9	7.2	−3.4	2.0	−0.8	−21.0

It is obvious from the tables that the cluster expansion of nucleon matter energy is not rapidly convergent with the optimum variational wave functions used here. In the case of SNM (Tables I and III) we evaluate the energy $E(x)$ at each density at 14 values of x and fit $E(x)-T_F-E_{\text{-}body}(x)$ by a polynomial having up to x^{12} to extract the (3–5)-body contributions with an accuracy of ~ 0.1 MeV. The cluster expansion for PNM at $\rho\leqslant\rho_0$ (Tables IV and V) converges more slowly than that for SNM. At higher-densities, PNM has two sets of minima indicating a phase transition. The higher-density phase (HDP) is expected to have neutral pion condensation [14]. The cluster expansion does not appear to be convergent in high-density neutron matter. The lower-density PNM results shown in Tables IV and V are obtained as for SNM and have similar accuracy, while those at $\rho\geqslant 1.5\rho_0$ use polynomials having up to x^{16}. The 3- and 4-body contributions in Tables VI–IX have accuracies of ~ 0.1 MeV, while the 5- and >5-body cluster contributions may have errors up to 0.5 MeV. However, their sum is correct within ~ 0.1 MeV in the FHNC/SOC approximation.

The contributions to v_{ij}^s and T_s alternate in sign as the number of bodies in the cluster increases, as expected from the chain equations. However, this is not necessarily the case for contributions to either v_{ij}^q or V_{ijk}. As mentioned earlier, there are additional 3-body terms that contribute to v_{ij}^q, and the short- and long-range parts of V_{ijk} have different behaviors, as will be discussed in Sec. IV.

In the present work we calculate the 3-body contributions, apart from the small v_{ij}^b and T_b terms, by an exact method described in the following section. It provides a direct test of the accuracy of SOC approximation for $n=3$. In nucleon matter, the 3-body cluster contribution is larger than the sum

TABLE II. Cluster contributions calculated with CSM: SNM at $\rho=\rho_0$, $\alpha=0.80$, $d_c=1.80$ fm, and $d_t=4.80$ fm, $T_F=22.1$ MeV, and $E_v^{CSM}=-8.9$ MeV.

n	2	3	4	5	>5	Total
v_{ij}^s	−66.7	11.1	−6.9	3.4	−1.1	−60.2
T_s	20.3	−2.0	2.4	−1.1	0.4	20.0
v_{ij}^q	4.5	3.5	0.2	0.0	0.0	8.1
V_{ijk}		1.9	1.0	0.3	−0.1	3.1
$v_{ij}^b+T_b$	−1.8	−0.1	−0.1	0	0	−2.0
$E_v^{CSM}-T_F$	−43.7	14.4	−3.4	2.6	−0.8	−31.0

TABLE III. Cluster contributions calculated with CSM: SNM at $\rho=1.5\rho_0$, $\alpha=0.89$, $d_c=1.50$ fm, and $d_t=3.99$ fm; $T_F=29.0$ and $E_v^{CSM}=-3.3$ MeV.

n	2	3	4	5	>5	Total
v_{ij}^s	−92.1	10.9	−6.2	2.8	−0.9	−85.5
T_s	28.7	−0.5	2.5	−0.8	0.2	30.1
v_{ij}^q	9.9	8.0	0.6	−0.1	−0.1	18.4
V_{ijk}		4.7	2.7	0.8	−0.3	7.9
$v_{ij}^b+T_b$	−2.7	−0.3	−0.1	0	0	−3.1
$E_v^{CSM}-T_F$	−56.2	22.8	−0.5	2.7	−1.1	−32.3

of all clusters with $n\geqslant 4$. Therefore we can hope that an improvement in the accuracy of the calculated energy can be achieved by using exact values of 2- and 3-body cluster energies, together with the CSM estimate for $n\geqslant 4$.

The main cause of the poor convergence of the PNM cluster expansion at $\rho\leqslant\rho_0$ is the long nn scattering length. As shown in Fig. 1 of AP, the energy of PNM at small density is very insensitive to the range of correlations, but the cluster expansion depends strongly on the range. Thus it is possible to use an F with smaller d_c and d_t and obtain essentially the same energy with a more convergent expansion, as will be discussed in more detail in Ref. [27].

III. EXACT CALCULATION OF 3-BODY CLUSTER CONTRIBUTION

Variational Monte Carlo calculations of light nuclei do not use an expansion in powers of spin-isospin correlations $f_{p\neq c}$. In that method [4] the 3-nucleon wave function is represented by a vector in spin-isospin space, and the F^s and v^s are matrix functions of interparticle distances. We first discuss the simpler case of PNM. We can eliminate the isospin dependence of v and F in PNM by setting all $\boldsymbol{\tau}_i\cdot\boldsymbol{\tau}_j=1$. The 3-neutron wave function is a vector of dimension $2^3=8$, whose components describe the amplitudes for each spin state, such as $\uparrow\uparrow\uparrow,\uparrow\uparrow\downarrow,\ldots$. The v_{ij}^s, F_{ij}^s, F_{jk}^s, and F_{ki}^s are 8×8 matrices, and Eq. (2.11) becomes

$$[v_{ij}^s-3b-\mathrm{dir}]=\frac{\rho^2}{2}\frac{1}{8}\int d^3r_{ij}d^3r_{ik}\mathrm{Tr}(\mathcal{M}v_{ij}^s\mathcal{M} - F_{ij}^s v_{ij}^s F_{ij}^s(F_{jk}^{s2}+F_{ki}^{s2}-1)). \quad (3.1)$$

TABLE IV. Cluster contributions calculated with CSM: PNM at $\rho=0.5\rho_0$, $\alpha=0.95$, $d_c=2.88$ fm, and $d_t=6.14$ fm; $T_F=22.1$ and $E_v^{CSM}=10.1$ MeV.

n	2	3	4	5	>5	Total
v_{ij}^s	−26.7	11.8	−9.4	7.2	−3.2	−20.3
T_s	7.3	−4.5	3.6	−2.8	1.3	4.9
v_{ij}^q	4.3	0.1	−0.2	0.1	0.0	4.4
V_{ijk}		1.5	−1.1	0.7	−0.1	1.0
$v_{ij}^b+T_b$	−2.0	0	0.1	0	0	−1.9
$E_v^{CSM}-T_F$	−17.0	8.9	−7.0	5.2	−2.0	−12.0

TABLE V. Cluster contributions calculated with CSM: PNM at $\rho=\rho_0$, $\alpha=0.95$,$d_c=2.74$ fm, and $d_t=4.39$ fm; $T_F=35.1$ and $E_v^{CSM}=19.0$ MeV.

n	2	3	4	5	>5	Total
v_{ij}^s	−48.5	17.8	−14.4	12.5	−6.0	−38.6
T_s	12.6	−6.6	5.3	−4.8	2.3	8.8
v_{ij}^q	12.9	1.3	−0.3	0.2	−0.1	14.0
V_{ijk}		7.2	−3.4	2.4	−0.6	5.6
$v_{ij}^b+T_b$	−5.9	0.2	0	0	0	−5.8
$E_v^{CSM}-T_F$	−29.0	19.9	−12.8	10.3	−4.4	−16.1

In uniform matter, the above six-dimensional spatial integral can be reduced to a three-dimensional integral over r_{ij}, r_{jk}, and r_{ki}, and evaluated using mesh points; in finite nuclei it is more convenient to use Monte Carlo methods for the spatial integrals. The above equation gives the sum of *all* 3-body direct diagrams containing v^s and F^s.

The antisymmetric bra $\langle\Phi_A(k_F)|$ in the expectation value [Eq. 2.8] is obtained by applying exchange operators to the $\langle\Phi_P(k_F)|$. Therefore in the contribution of exchange diagrams, the spin exchange operators,

$$e_{ij}=-\frac{1}{2}(1+\boldsymbol{\sigma}_i\cdot\boldsymbol{\sigma}_j), \quad (3.2)$$

appear to the left of all the F^s operators. Note that e_{ij} is also an 8×8 matrix in the spin vector space. The sum of *all* 3-body diagrams with nucleons ij exchanged is given by

$$[v_{ij}^s-3b-e_{ij}]=\frac{\rho^2}{2}\frac{1}{8}\int d^3r_{ij}\ d^3r_{ik}\ l^2(r_{ij}) \times\mathrm{Tr}(e_{ij}\mathcal{M}v_{ij}^s\mathcal{M}-e_{ij}F_{ij}^s v_{ij}^s F_{ij}^s \times(F_{jk}^{s2}+F_{ki}^{s2}-1)). \quad (3.3)$$

The Slater function takes into account the spatial exchange of each particle.

The diagrams with jk or ik exchanged give identical contribution. Their sum is given by

TABLE VI. Cluster contributions calculated with CSM: PNM at $\rho=1.5\rho_0$, $\alpha=0.83$, $d_c=2.99$ fm, and $d_t=3.30$ fm; $T_F=46.0$ and $E_v^{CSM}=33.4$ MeV.

n	2	3	4	5	>5	Total
v_{ij}^s	−68.9	25.5	−24.6	30.0	−17.0	−55.0
T_s	17.6	−9.3	8.5	−10.6	5.8	12.0
v_{ij}^q	22.2	3.9	−0.5	0.4	−0.1	25.9
V_{ijk}		19.3	−9.2	7.5	−2.6	15.0
$v_{ij}^b+T_b$	−10.1	0	−0.2	0.2	−0.2	−10.4
$E_v^{CSM}-T_F$	−39.2	39.4	−26.0	27.5	−14.1	−12.5

TABLE VII. Cluster contributions calculated with CSM: PNM at $\rho=2\rho_0$, $\alpha=0.87$, $d_c=2.86$ fm, and $d_t=2.86$ fm; $T_F=55.7$ and $E_v^{CSM}=55.0$ MeV.

n	2	3	4	5	>5	Total
v_{ij}^s	−86.5	22.9	−21.9	26.8	−14.5	−73.2
T_s	21.4	−7.6	6.9	−9.0	4.7	16.4
v_{ij}^q	34.4	8.4	0.5	0.2	0.0	43.5
V_{ijk}		33.2	−9.2	11.1	−5.6	29.5
$v_{ij}^b+T_b$	−15.6	−0.3	−0.9	0.4	−0.4	−16.8
$E_v^{CSM}-T_F$	−46.2	56.6	−24.6	29.5	−15.8	−0.6

$$[v_{ij}^s-3b-(e_{jk}+e_{ki})]=\rho^2\frac{1}{8}\int d^3r_{ij}d^3r_{ik}l^2(r_{ik}) \times \mathrm{Tr}(e_{ki}\mathcal{M}v_{ij}^s\mathcal{M}-F_{ij}^s v_{ij}^s F_{ij}^s e_{ki}F_{ki}^{s2}). \tag{3.4}$$

In addition, there are two 3-body circular exchange diagrams. The $\langle\Phi_P(k_F)|e_{jk}e_{ij}$ produces the state in which nucleon i occupies the state of j in $|\Phi_P(k_F)\rangle$, j that of k, and k that of i. We denote this exchange by $i\to j\to k\to i$. The $\langle\Phi_P(k_F)|e_{ij}e_{jk}$ produces the other cyclic exchange in which $i\to k\to j\to i$. Both cyclic exchanges give the same contribution. Their sum is

$$[v_{ij}^s-3b-\mathrm{cir}]=\rho^2\frac{1}{8}\int d^3r_{ij}d^3r_{ik}l(r_{ij})l(r_{jk})l(r_{ki}) \times \mathrm{Tr}(e_{jk}e_{ij}\mathcal{M}v_{ij}^s\mathcal{M}-e_{ij}F_{ij}^s v_{ij}^s F_{ij}^s\ e_{ki} \times (F_{ki}^{s2}-1)). \tag{3.5}$$

Here we have used

$$\langle\Phi_P(k_F)|e_{jk}e_{ij}=\langle\Phi_P(k_F)|e_{ij}e_{ki}. \tag{3.6}$$

The entire 3-body cluster contribution to the expectation value of v^s including only F^s correlations is given by the sum of the direct, e_{ij}, e_{jk}, e_{ki} and circular exchange contributions given above *without any approximation*.

The 3-body cluster contribution to $\langle V_{ijk}\rangle$ is rather simple in this representation. Since it is the leading term, there are no subtractions as in Eqs. (3.1) and (3.3)–(3.5) for $[v_{ij}^s-3b]$. The $[V_{ijk}-3b]$ contributions are obtained by keeping only the first term in the traces in these equations, and replacing the v_{ij}^s by $V_{ijk}/3$.

TABLE VIII. Cluster contributions calculated with CSM: PNM HDP at $\rho=1.5\rho_0$, $\alpha=1.36$, $d_c=1.70$ fm, and $d_t=4.94$ fm; $T_F=46.0$ and $E_v^{CSM}=35.2$ MeV.

n	2	3	4	5	>5	Total
v_{ij}^s	−69.7	13.7	−15.0	10.9	−6.2	−66.3
T_s	19.4	−4.0	6.1	−3.3	2.0	20.2
v_{ij}^q	28.0	6.6	0.3	−1.1	−0.2	33.6
V_{ijk}		7.3	−0.2	2.5	−0.7	8.9
$v_{ij}^b+T_B$	−9.3	0.6	0.9	0.5	0.1	−7.2
$E_v^{CSM}-T_F$	−31.6	24.2	−7.9	9.5	−5.0	−10.8

TABLE IX. Cluster contributions calculated with CSM: PNM HDP at $\rho=2\rho_0$, $\alpha=1.26$, $d_c=1.68$ fm, and $d_t=4.48$ fm; $T_F=55.7$ and $E_v^{CSM}=52.6$ MeV.

n	2	3	4	5	>5	Total
v_{ij}^s	−89.4	11.2	−11.6	7.0	−4.9	−87.7
T_s	23.1	−2.8	4.4	−1.3	1.4	24.8
v_{ij}^q	40.3	13.1	1.0	−1.8	−.5	52.1
V_{ijk}		15.9	2.0	4.9	−3.1	19.7
$v_{ij}^b+T_b$	−13.3	−0.3	0.5	0.7	0.3	−12.1
$E_v^{CSM}-T_F$	−39.3	37.1	−3.7	9.5	−6.8	−3.1

The kinetic energy has terms containing $\nabla_i^2\mathcal{M}$, and $\boldsymbol{\nabla}_i\mathcal{M}\cdot\boldsymbol{\nabla}_i|\Phi_P(k_F)\rangle$. The $|\Phi_P(k_F)\rangle$ is an eigenstate of ∇_i^2. The sum of all terms having $\nabla_i^2|\Phi_P(k_F)\rangle$ gives the Fermi-gas kinetic energy T_F. Therefore these terms are not included in the cluster expansion of $E-T_F$. It can be verified that all the terms having $\nabla_i^2\mathcal{M}$ are obtained from Eqs. (3.1) and (3.3)–(3.5), with the substitutions

$$v_{ij}^s\mathcal{M}\to -2[\mathcal{S}(\nabla_i^2\ F_{ij}^s)F_{jk}^sF_{ki}^s] -2[\mathcal{S}(\boldsymbol{\nabla}_iF_{ij}^s)\cdot(\boldsymbol{\nabla}_iF_{ki}^s)F_{ki}^s] \tag{3.7}$$

in the first term of the trace and

$$v_{ij}^sF_{ij}^s\to -2(\nabla_i^2F_{ij}^s), \tag{3.8}$$

in the second term. Terms containing $\boldsymbol{\nabla}_iF_{ij}^s\cdot\boldsymbol{\nabla}_iF_{ki}^s$ are denoted by u, while those with $\nabla_i^2\ F_{ij}^s$ are included in w in FHNC-SOC calculations [20].

Terms containing $\boldsymbol{\nabla}_i|\Phi_P(k_F)\rangle=i\mathbf{k}_i|\Phi_P(k_F)\rangle$ give zero contribution in direct diagrams after summation over $\mathbf{k}_i$. These terms contribute only via exchange diagrams in which the $\Sigma_i i\mathbf{k}_ie^{i\mathbf{k}_i\cdot\mathbf{r}_{ij}}$ gives $l'(r_{ij})\hat{\mathbf{r}}_{ij}$, where $\hat{\mathbf{r}}_{ij}$ denotes the unit vector. The $\boldsymbol{\nabla}_i\mathcal{M}\cdot\boldsymbol{\nabla}_i|\Phi_P(k_F)\rangle$ contributions are classified as follows [20]. Let $\boldsymbol{\nabla}_i$ operate on F_{ij}^s in $\mathcal{M}$; this defines the nucleon j. Exchange diagrams in which $i\to j$ are called w_F; they contain $l'(r_{ij})\hat{\mathbf{r}}_{ij}$, and give

$$[w_F-3b-e_{ij}]=-\frac{1}{m}\frac{\rho^2}{8}\int d^3r_{ij}d^3r_{ki}l(r_{ij})l'(r_{ij})\hat{\mathbf{r}}_{ij} \times \mathrm{Tr}(e_{ij}\mathcal{M}[\mathcal{S}(\boldsymbol{\nabla}_iF_{ij}^s)F_{jk}^sF_{ki}^s] -e_{ij}(F_{ij}^s\boldsymbol{\nabla}_iF_{ij}^s)(F_{jk}^{s2}+F_{ki}^{s2}-1)), \tag{3.9}$$

$$[w_F-3b-\mathrm{cir}]=-\frac{1}{m}\frac{\rho^2}{8}\int d^3r_{ij}d^3r_{ki}l(r_{jk})l(r_{ki})l'(r_{ij})\hat{\mathbf{r}}_{ij} \times \mathrm{Tr}(e_{jk}e_{ij}\mathcal{M}[\mathcal{S}(\boldsymbol{\nabla}_iF_{ij}^s)F_{jk}^sF_{ki}^s] -e_{ij}(F_{ij}^s\boldsymbol{\nabla}_iF_{ij}^s)e_{ki}F_{ki}^{s2}). \tag{3.10}$$

These contain subtracted terms from the denominator expansion, since w_F has a 2-body cluster contribution from $e_{ij}l(r_{ij})l'(r_{ij})\hat{\mathbf{r}}_{ij}\cdot(F^s_{ij}\boldsymbol{\nabla}_i F^s_{ij})$.

The contribution of terms in which $i\rightarrow k\neq j$ in the exchange loop are called u_F, and

$$[u_F-3b-e_{ki}]=-\frac{1}{m}\frac{\rho^2}{8}\int d^3r_{ij}d^3r_{ki}l(r_{ki})l'(r_{ki})\hat{\mathbf{r}}_{ki}\times\mathrm{Tr}(e_{ki}\mathcal{M}[\mathcal{S}(\boldsymbol{\nabla}_i F^s_{ij})F^s_{jk}F^s_{ki}]-e_{ki}F^s_{ij}\boldsymbol{\nabla}_i F^s_{ij}(F^{s2}_{ik}-1)), \tag{3.11}$$

$$[u_F-3b-\mathrm{cir}]=-\frac{1}{m}\frac{\rho^2}{8}\int d^3r_{ij}d^3r_{ki}l(r_{ij})l(r_{jk})l'(r_{ik})\hat{\mathbf{r}}_{ik}\times\mathrm{Tr}(e_{ij}e_{jk}\mathcal{M}[\mathcal{S}(\boldsymbol{\nabla}_i F^s_{ij})F^s_{jk}F^s_{ki}]-e_{ij}(F^s_{ij}\boldsymbol{\nabla}_i F^s_{ij})e_{jk}). \tag{3.12}$$

The u_F diagrams must have at least three nucleons, i,j, and k. There are no 2-body u_F diagrams, and thus there are no denominator subtractions in u_F-3b. The subtracted terms in the above two equations are, in fact, zero; that in Eq. (3.11) has zero integral over the angle between $\mathbf{r}_{ki}$ and $\boldsymbol{\nabla}_i F^s_{ij}$, while that in Eq. (3.12) has uncorrelated nucleon k in an exchange loop. However, the subtractions help to restrict the domain of integrals over r_{jk} and r_{ki} which are otherwise large.

The equations for the v^q-3b contributions are given in Appendix A, and the numerical methods used for the exact calculation of 3-body v^s_{ij}, T_s, V_{ijk}, and v^q_{ij} are described in Appendix B.

The PNM formalism can also be used for SNM. However, the number of 3-nucleon spin-isospin states is 64, and thus all the F's and interactions are 64×64 matrix functions of the $\mathbf{r}_i,\mathbf{r}_j$, and $\mathbf{r}_k$ in this formalism. In PNM they are only 8×8 matrix functions. A more efficient way to calculate the 3-body cluster in SNM is as follows.

The pair correlations and the interactions can be separated into parts that contain and do not contain isospin operators as follows:

$$F^s_{ij}=F^0_{ij}+F^\tau_{ij}\boldsymbol{\tau}_i\cdot\boldsymbol{\tau}_j,$$
$$F^0_{ij}=f^c_{ij}+f^\sigma_{ij}\boldsymbol{\sigma}_i\cdot\boldsymbol{\sigma}_j+f^t_{ij}S_{ij},$$
$$F^\tau_{ij}=f^\tau_{ij}+f^{\sigma\tau}_{ij}\boldsymbol{\sigma}_i\cdot\boldsymbol{\sigma}_j+f^{t\tau}_{ij}S_{ij}. \tag{3.13}$$

Both F^0 and F^τ operate only on the spins and are 8×8 matrix functions. In nnn and ppp clusters, $\boldsymbol{\tau}_i\cdot\boldsymbol{\tau}_j=1$. These clusters have only eight spin-isospin states, and there contributions are calculated as in PNM using $F^0_{ij}+F^\tau_{ij}$ in place of F^0_{ij}.

Clusters with two neutrons and a proton have three isospin states denoted by nnp,npn, and pnn. In these clusters we treat the F^s_{ij} as a 3×3 matrix whose elements are combinations of 8×8 matrix functions F^0 and F^τ. For example, the 3×3 matrix representation of F^s_{ij} is

$$F^s_{ij}=\begin{pmatrix}F^0_{ij}+F^\tau_{ij} & 0 & 0\\ 0 & F^0_{ij}-F^\tau_{ij} & 2F^\tau_{ij}\\ 0 & 2F^\tau_{ij} & F^0_{ij}-F^\tau_{ij}\end{pmatrix}. \tag{3.14}$$

This matrix operates on the wave function vector:

$$\boldsymbol{\Psi}_{ijk}=\begin{pmatrix}\psi_{ijk=nnp}(\mathbf{r}_i,\mathbf{r}_j,\mathbf{r}_k)\\ \psi_{ijk=npn}(\mathbf{r}_i,\mathbf{r}_j,\mathbf{r}_k)\\ \psi_{ijk=pnn}(\mathbf{r}_i,\mathbf{r}_j,\mathbf{r}_k)\end{pmatrix}, \tag{3.15}$$

where $\psi_{ijk=nnp}(\mathbf{r}_i,\mathbf{r}_j,\mathbf{r}_k)$, for example, is an eight component spin wave function in which i and j are neutrons and k is a proton. We need to calculate only the 3-neutron and the 2-neutron−1-proton cluster contributions in SNM since they do not change on interchanging all protons with neutrons.

IV. RESULTS

The results of exact 3-body cluster contributions in SNM and PNM are compared with those obtained with the CSM in Tables X and XI. The FHNC sums include all the contributions containing central correlations without approximation; however, the 3-body contribution is dominated by spin-isospin correlations. The difference between the exact and the CSM results is entirely due to truncations in the number of spin-isospin correlations included in the SOC. In SNM the 3-body estimate of CSM is larger than the exact result by 44%, 33%, and 22% at $0.5\rho_0$, $1.0\rho_0$, and $1.5\rho_0$, while in the low-density phase of PNM it is smaller by only 8%, 6%, and 4% at these densities. At higher densities the chain diagrams become more important and the CSM becomes more accurate. This is rather fortunate because in high-density PNM the cluster expansion is not convergent, and one has to rely on integral equations to sum all of the clusters. The larger error in CSM in SNM is due to the strong tensor correlations in $T=0,S=1$ channels. When the tensor correlations are switched off, the 3-body CSM and exact energies are 8.4 and 7.7 MeV at ρ_0. However, in this case the $E_V>0$, since nuclear matter is not bound in the absence of tensor correlations.

There is a large cancellation between the two terms of the Urbana IX V_{ijk} in SNM. The spin-isospin independent term V^R is repulsive and CSM estimates its contribution fairly accurately. In contrast, the Fujita-Miyazawa interaction $V^{2\pi}_{ijk}$

TABLE X. The 3-body cluster contribution from F^s correlations calculated exactly and with CSM for SNM in MeV.

	$0.5\rho_0$		ρ_0		$1.5\rho_0$	
	Exact	CSM	Exact	CSM	Exact	CSM
T_s	−1.8	−1.6	−2.5	−2.0	−1.1	−0.5
v^s_{ij}	5.7	7.4	9.3	11.1	10.4	10.9
v^q_{ij}	0.9	0.8	3.2	3.5	6.3	8.0
V^R_{ijk}	1.7	1.6	6.3	6.0	13.7	13.3
$V^{2\pi}_{ijk}$	−1.6	−1.0	−5.4	−4.1	−10.2	−8.6
Total 3b	5.0	7.2	10.9	14.5	19.0	23.1

TABLE XI. The 3-body cluster contribution from F^s correlations calculated exactly and with CSM for PNM in MeV.

	$0.5\rho_0$		ρ_0		$1.5\rho_0$	
	Exact	CSM	Exact	CSM	Exact	CSM
T_s	−4.2	−4.5	−6.3	−6.6	−9.4	−9.3
v_{ij}^s	11.8	11.8	17.9	17.8	25.7	25.5
v_{ij}^q	0.3	0.1	1.3	1.3	4.3	3.9
V_{ijk}^R	1.4	1.4	6.6	6.5	16.7	16.3
$V_{ijk}^{2\pi,FMA}$	0.5	0.2	1.4	0.7	3.9	2.9
Total 3b	9.8	9.0	20.9	19.7	41.1	39.4
	$2\rho_0$		HDP $1.5\rho_0$		HDP $2\rho_0$	
	Exact	CSM	Exact	CSM	Exact	CSM
T_s	−8.2	−7.6	−3.1	−4.0	−1.9	−2.8
v_{ij}^s	23.2	22.9	14.0	13.7	11.6	11.2
v_{ij}^q	7.3	8.4	5.8	6.6	10.0	13.1
V_{ijk}^R	29.0	28.7	11.4	11.6	21.4	21.7
$V_{ijk}^{2\pi,FMA}$	5.6	4.4	−2.4	−4.3	−3.6	−5.8
Total 3b	56.8	56.9	25.6	25.0	37.4	38.6

is entirely spin-isospin dependent, and the CSM is less accurate in calculating its 3-body contribution. Thus the total V_{ijk} expectation value can have a relatively large error in the CSM.

As can be seen from Table XI, the 3-body cluster contribution increases rapidly with density in the low-density phase of PNM in which the $V_{ijk}^{2\pi}$ is repulsive. In the HDP, $V_{ijk}^{2\pi}$ becomes attractive and reduces the 3-body contribution significantly. The CSM has fair accuracy in evaluating the 3-body cluster contribution in both the phases of PNM.

We can hope to get more accurate evaluations of the energy expectation value by summing the Fermi kinetic energy T_F, the 2-body, and the matrix 3-body cluster energies. These terms are large and are calculated exactly. The remainder, denoted by ΔE, includes $\geqslant$4-body clusters with F^s correlations and $\geqslant$3-body clusters with v^b and/or F^b, and is estimated with CSM. The variational energies obtained in this way are listed in Tables XII and XIII. In SNM they are significantly below the results obtained earlier using CSM for all $n\geqslant$3-body (3b) cluster. The new PNM energies are closer to the older results. The approximately calculated ΔE is relatively small for the sum of Argonne $v18+$Urbana IX interactions, and if the error in ΔE is less than 25% (the accuracy of CSM for 3-body cluster), the calculated E_V's will have less than 10% error. However, it is difficult to estimate the error in ΔE since there are cancellations between the contributions of 4-, 5- and $>$5-body clusters.

TABLE XII. Variational energy of SNM obtained with the exact 3-body cluster contribution in MeV. The last column gives the value obtained with CSM.

ρ	T_F	E-2b	E-3b-F^s	ΔE	E_V	E_V^{CSM}
$0.5\rho_0$	13.9	−25.9	4.9	−2.2	−9.3	−7.1
ρ_0	22.1	−43.7	10.9	−1.7	−12.4	−8.9
$1.5\rho_0$	29.0	−56.2	19.1	0.8	−7.3	−3.3

V. CONCLUSIONS AND OUTLOOK

At present we can calculate the 1-, 2-, and most of 3-body cluster contributions, T_F, E-2b and E-3b-F^s to the energy of nucleon matter exactly with realistic variational wave functions. However, the cluster expansion is not rapidly convergent in variational theories of nucleon matter, and it is necessary to use CSM to estimate the rest of the contributions denoted by ΔE. For example, at the equilibrium density, the 1–5-body cluster contributions to the energy of SNM are 22.1, −43.7, 10.8, −3.4, and 2.6 MeV, while those with $n>5$ give −0.8 MeV. Of these the first three are now calculated exactly, apart from the small 3-body spin-orbit contribution (see Table III). The $n\geqslant$4-body are approximate CSM estimates; they add up to −1.6 MeV.

For some Hamiltonians, such as the present one, T_F, E-2b and E-3b are all comparable to or larger in magnitude than

TABLE XIII. Variational energy of PNM obtained with the exact 3-body cluster contribution in MeV. The last column gives the value obtained with CSM.

ρ	T_F	E-2b	E-3b-F^s	ΔE	E_V	E_V^{CSM}
$0.5\rho_0$	22.1	−17.0	9.8	−3.8	11.1	10.1
ρ_0	35.1	−29.0	20.9	−6.7	20.3	19.0
$1.5\rho_0$	46.0	−39.2	41.2	−12.6	35.4	33.4
$2\rho_0$	55.7	−46.2	56.8	−11.2	55.1	55.0
$1.5\rho_0$ HDP	46.0	−31.5	25.6	−2.8	37.3	35.2
$2\rho_0$ HDP	55.7	−39.3	37.4	−1.3	52.5	52.6

E_V. For these it is probably essential to calculate the E-3b exactly. The error in E_V is then due to that in the CSM estimate of ΔE. It is not well known, however, the fractional error in the CSM estimate of ΔE is likely to be larger than that in the CSM estimate of E-3b, which is $\sim$33% in SNM at ρ_0 (Table X).

We obtain significantly more binding for SNM with the present calculations. In the earlier CSM calculations, the SNM $E_V^{CSM}(\rho_0)=-9.4$ MeV (see Table II of AP). The present value of $E_V^{CSM}(\rho_0)=-8.9$ MeV, listed in Table II, is higher due to the chain dressings added to 3-body diagrams with v^q. The $E(\rho_0)=-12.0$ MeV estimated by AP is obtained by adding to the $E_V^{CSM}(\rho_0)$ half the difference of the kinetic energies obtained with the Pandharipande-Bethe and Jackson-Feenberg [28] expressions ($=-0.6$), and a perturbative correction ($=-1.9$ MeV) for the limitations of the present variational wave function. Adding the perturbative correction to the present $E_V(\rho_0)=-12.4$ (Table XII), we obtain $E(\rho_0)\sim-14$ MeV, much closer to the empirical value of -16 MeV. It now appears possible that accurate calculations of SNM with more realistic interaction models, including 3-pion exchange terms in V_{ijk} [2], can provide adequate binding to SNM.

It is interesting to note that Fabrocini *et al.* [29] also find that the FHNC/SOC calculations underestimate the binding energy of ^{16}O nucleus by $\sim$1 MeV per nucleon, compared with the energy obtained with the cluster Monte Carlo method [30]. In the latter method contributions of up to 4-body clusters are calculated exactly, except for spin-orbit correlations.

The CSM calculations are computationally simple: it takes only $\sim$10 sec to calculate the SNM E_V^{CSM} on a workstation operating at $\sim$150 MFLOPS. The present calculation of E_V takes $\sim$10 min instead. Using Monte Carlo integration methods, as in the calculation of ^{16}O [30], it may be possible to calculate 4- and possibly 5-body clusters with negligible errors using F^s alone. Such calculations will include the leading elementary diagrams, and will be valuable for SNM near equilibrium density, where the contribution of >5-body clusters is estimated to be very small with the present Ψ_V. They will need much larger computational resources, which are fortunately now available.

Near the indicated phase transition in PNM, the contribution of >5-body clusters is not small. Here the cluster expansion does not appear to be convergent. If we define ΔE_n as the sum of all clusters with $>n$ bodies, from Table IX we obtain the CSM estimates of $\Delta E_n=36.2,\ -0.9,\ 2.7$, and -6.8 MeV for $n=2,3,4$, and 5. Fortunately, in this case the CSM estimate of E-3b-F^s of 38.6 MeV is close to the exact value of 37.4 MeV (Table X). An exact calculation of E-4b may not improve the accuracy of the total E_V here, although it will provide an important additional test of the accuracy of CSM.

It is also necessary to have improved estimates of contributions of clusters with v^b and/or F^b for better accuracy of the calculated E_V. Even though the present estimates of >2-body contributions of v^b and F^b are rather small (Tables I–IX), these are more approximate. For example, they do not include all the FHNC/SOC diagrams summed in CSM.

The cluster expansion depends sensitively on the Hamiltonian. For example, the problem of SNM has been studied by many groups using the older Argonne $v14$ interaction without any V_{ijk}. In his classic Brueckner theory calculations, Day [11] obtained an energy of -17.8 ± 1.3 for SNM at $k_F=1.6$ fm^{-1} or $\rho=1.73\rho_0$. The present calculation gives a lower energy in this case. The values obtained for T_F, E-2b, E-3b-F^s, and ΔE are, respectively, 31.9, -61.2, 10.2, and -3.2, giving a total of -22.3 MeV. However, the CSM is not very accurate in this case. The estimate of E-3b-F^s with CSM is 19.0 MeV, too large by a factor of 2. The CSM estimate of ΔE could also have a large error in this case. In such cases it is probably necessary to have complete calculations of 4- and possibly 5-body clusters to obtain reliable estimates of E_V.

ACKNOWLEDGMENTS

The authors thank Dr. M. W. Paris, Dr. S. C. Pieper, and Dr. R. B. Wiringa for useful discussions and comments. This work has been partly supported by the US National Science Foundation via Grant No. PHY 00-98353.

APPENDIX A: EXPECTATION VALUES OF QUADRATIC INTERACTIONS

Interactions containing L^2 or $(\mathbf{L}\cdot\mathbf{S})^2$ operators are expressed in the form

$$v^{L^2,p}(r_{12})O_{12}^p L^2=(\mathbf{r}_{12}\times\boldsymbol{\nabla}')\cdot X_{12}^p(\mathbf{r}_{12}\times\boldsymbol{\nabla}), \tag{A1}$$

$$X_{12}^p=v^{L^2,p}(r_{12})O_{12}^p, \tag{A2}$$

$$v^{(\mathbf{L}\cdot\mathbf{S})^2,p}(r_{12})O_{12}^p(\mathbf{L}\cdot\mathbf{S})^2=(\boldsymbol{\nabla}'\cdot\mathbf{S}\times\mathbf{r}_{12})Y_{12}^p(\mathbf{S}\times\mathbf{r}_{12}\cdot\boldsymbol{\nabla}), \tag{A3}$$

$$Y_{12}^p=v^{(\mathbf{L}\cdot\mathbf{S})^2,p}(r_{12})O_{12}^p. \tag{A4}$$

Here $\boldsymbol{\nabla}=(\boldsymbol{\nabla}_1-\boldsymbol{\nabla}_2)/2$ operates to the right on the Ψ, while $\boldsymbol{\nabla}'$ operates to the left on the $\Psi^\dagger$. The O^p in L^2 terms can be $(1,\boldsymbol{\sigma}_1\cdot\boldsymbol{\sigma}_2)\otimes(1,\boldsymbol{\tau}_1\cdot\boldsymbol{\tau}_2)$, while those in $(\mathbf{L}\cdot\mathbf{S})^2$ terms can only be 1 or $\boldsymbol{\tau}_1\cdot\boldsymbol{\tau}_2$. The X_{12}^p and Y_{12}^p are known matrix functions of r_{12}.

The $\boldsymbol{\nabla}$ can operate on either the correlation operators or the plane waves in Φ. For brevity, we define

$$\boldsymbol{\nabla}\mathcal{M}=\mathcal{M}\boldsymbol{\nabla}'=\mathbf{M}. \tag{A5}$$

On the right-hand, side we use a simple product Φ_P, and

$$\boldsymbol{\nabla}\Phi_P=\frac{i}{2}(\mathbf{k}_1-\mathbf{k}_2)\Phi_P. \tag{A6}$$

However, the $\Phi_A^\star\boldsymbol{\nabla}'$ depends upon the exchange pattern. The essential problem in computing these contributions is that of summing over the $\mathbf{k}_{i=1,2,3}$ in the exchange diagrams. All the contributions can be expressed as

$$\frac{\rho^2}{2}\frac{1}{8}\int d^3r_{ij}\ d^3r_{ik}\mathrm{Tr}\mathcal{I}^X, \tag{A7}$$

where $X=D$ for direct, C for circular exchange, A for e_{12}, and B for e_{13} and e_{23} pair exchange diagrams. Each $\mathcal{I}^X$ can be expressed as

$$\mathcal{I}^X=\mathcal{I}^X_{FF}+\mathcal{I}^X_{FK}+\mathcal{I}^X_{KK}, \tag{A8}$$

where the subscripts FF, FK, and KK denote terms in which both, one, and none of the gradients operate on the correlation operators. In FF terms, the sums over momenta $\mathbf{k}_{i=1,2,3}$ can be easily zcarried out to obtain Slater functions. The FK terms are zero for the direct and e_{12} diagrams, and were neglected in the earlier calculations of AP and APR. In these and KK terms, one obtains derivatives of Slater functions or k_F^2 from sums over plane wave momenta. We give below the $\mathcal{I}$ for PNM. Those for SNM have a similar structure.

1. Direct diagrams

In these diagrams $\Phi^\star\nabla'=\Phi^\star(-i)(\mathbf{k}_1-\mathbf{k}_2)/2$. The $\mathcal{I}^D$ for L^2 terms are given by

$$\mathcal{I}^D_{FF}=(\mathbf{r}_{12}\times\mathbf{M})\cdot X^p_{12}\ (\mathbf{r}_{12}\times\mathbf{M})-(\mathbf{r}_{12}\times\nabla F^s_{12})\cdot X^p_{12}\times(\mathbf{r}_{12}\times\nabla F^s_{12})(F^{s2}_{23}+F^{s2}_{31}-1), \tag{A9}$$

$$\mathcal{I}^D_{FK}=0, \tag{A10}$$

$$\mathcal{I}^D_{KK}=\frac{1}{5}r^2_{12}k^2_F\times(\mathcal{M}X^p_{12}\mathcal{M}-F^s_{12}X^p_{12}F^s_{12}(F^{s2}_{23}+F^{s2}_{31}-1)), \tag{A11}$$

while those for the $(\mathbf{L}\cdot\mathbf{S})^2$ are

$$\mathcal{I}^D_{FF}=(\mathbf{M}\cdot\mathbf{S}\times\mathbf{r}_{12})\cdot Y^p_{12}\ (\mathbf{S}\times\mathbf{r}_{12}\cdot\mathbf{M})-(\nabla F^s_{12}\cdot\mathbf{S}\times\mathbf{r}_{12})\cdot Y^p_{12}(\mathbf{S}\times\mathbf{r}_{12}\cdot\nabla F^s_{12})\times(F^{s2}_{23}+F^{s2}_{31}-1), \tag{A12}$$

$$\mathcal{I}^D_{FK}=0, \tag{A13}$$

$$\mathcal{I}^D_{KK}=\frac{1}{10}k^2_F(\mathcal{M}(\mathbf{S}\times\mathbf{r}_{12})\cdot Y^p_{12}\ (\mathbf{S}\times\mathbf{r}_{12})\mathcal{M}-F^s_{12}(\mathbf{S}\times\mathbf{r}_{12})\cdot Y^p_{12}\ (\mathbf{S}\times\mathbf{r}_{12})\times F^s_{12}(F^{s2}_{23}+F^{s2}_{31}-1)). \tag{A14}$$

2. Pair exchange diagrams

In e_{12} diagrams, $\Phi^\star\nabla'=\Phi^\star(i)(\mathbf{k}_1-\mathbf{k}_2)/2$. The $\mathcal{I}^A$ for L^2 terms are given by

$$\mathcal{I}^A_{FF}=e_{12}l^2(r_{12})((\mathbf{r}_{12}\times\mathbf{M})\cdot X^p_{12}\ (\mathbf{r}_{12}\times\mathbf{M})-(\mathbf{r}_{12}\times\nabla F^s_{12})\cdot X^p_{12}\ (\mathbf{r}_{12}\times\nabla F^s_{12})(F^{s2}_{23}+F^{s2}_{31}-1)), \tag{A15}$$

$$\mathcal{I}^A_{FK}=0, \tag{A16}$$

$$\mathcal{I}^A_{KK}=e_{12}r_{12}l(r_{12})l'(r_{12})\times(\mathcal{M}\ X^p_{12}\ \mathcal{M}-F^s_{12}X^p_{12}F^s_{12}(F^{s2}_{23}+F^{s2}_{31}-1)), \tag{A17}$$

while those for the $(\mathbf{L}\cdot\mathbf{S})^2$ are

$$\mathcal{I}^A_{FF}=e_{12}l^2(r_{12})((\mathbf{M}\cdot\mathbf{S}\times\mathbf{r}_{12})\cdot Y^p_{12}\ (\mathbf{S}\times\mathbf{r}_{12}\cdot\mathbf{M})-(\nabla F^s_{12}\cdot\mathbf{S}\times\mathbf{r}_{12})\cdot Y^p_{12}(\mathbf{S}\times\mathbf{r}_{12}\cdot\nabla F^s_{12})(F^{s2}_{23}+F^{s2}_{31}-1)), \tag{A18}$$

$$\mathcal{I}^A_{FK}=0, \tag{A19}$$

$$\mathcal{I}^A_{KK}=e_{12}\frac{l(r_{12})l'(r_{12})}{2r_{12}}\times(\mathcal{M}\ (\mathbf{S}\times\mathbf{r}_{12})\cdot Y^p_{12}\ (\mathbf{S}\times\mathbf{r}_{12})\mathcal{M}-F^s_{12}(\mathbf{S}\times\mathbf{r}_{12})\cdot Y^p_{12}\ (\mathbf{S}\times\mathbf{r}_{12})F^s_{12}(F^{s2}_{23}+F^{s2}_{31}-1)). \tag{A20}$$

In e_{13} diagrams, $\Phi^\star\nabla'=\Phi^\star(-i)(\mathbf{k}_3-\mathbf{k}_2)/2$. In the following equations, their contribution is doubled to take into account that of e_{23} diagrams. The $\mathcal{I}^B$ for L^2 terms are given by

$$\mathcal{I}^B_{FF}=2e_{13}l^2(r_{13})((\mathbf{r}_{12}\times\mathbf{M})\cdot X^p_{12}\ (\mathbf{r}_{12}\times\mathbf{M}))-2(\mathbf{r}_{12}\times\nabla F^s_{12})\cdot X^p_{12}\ (\mathbf{r}_{12}\times\nabla F^s_{12})e_{13}F^{s2}_{13}\ l^2(r_{13}), \tag{A21}$$

$$\mathcal{I}^B_{FK}=e_{13}\frac{l(r_{13})l'(r_{13})}{r_{13}}((\mathbf{r}_{12}\times\mathbf{M})X^p_{12}\cdot(\mathbf{r}_{12}\times\mathbf{r}_{13})\mathcal{M}+\mathcal{M}(\mathbf{r}_{12}\times\mathbf{r}_{13})X^p_{12}\cdot(\mathbf{r}_{12}\times\mathbf{M}))-\frac{l(r_{13})l'(r_{13})}{r_{13}}((\mathbf{r}_{12}\times\nabla F^s_{12})\times X^p_{12}\cdot(\mathbf{r}_{12}\times\mathbf{r}_{13})F^s_{12}-F^s_{12}(\mathbf{r}_{12}\times\mathbf{r}_{13})X^p_{12}\cdot(\mathbf{r}_{12}\times\nabla F^s_{12}))e_{13}F^{s2}_{13}, \tag{A22}$$

$$\mathcal{I}^B_{KK}=2e_{13}r_{12}^2\left(\frac{1}{10}k_F^2l^2(r_{13})+\frac{1}{4}l'^2(r_{13})[1-(\hat{\mathbf{r}}_{12}\cdot\hat{\mathbf{r}}_{13})^2]\right)(\mathcal{M}\ \ X^p_{12}\ \ \mathcal{M})-F^s_{12}X^p_{12}F^s_{12}r_{12}^2\left(\frac{l^2(r_{13})}{5}k_F^2-\frac{1}{2}l''(r_{13})l(r_{13})\right.$$
$$\left.\times[1-(\hat{\mathbf{r}}_{12}\cdot\hat{\mathbf{r}}_{13})^2]-\frac{l'(r_{13})l(r_{13})}{2r_{13}}[1+(\hat{\mathbf{r}}_{12}\cdot\hat{\mathbf{r}}_{13})^2]\right)e_{13}F^{s2}_{13}, \tag{A23}$$

while those for $(\mathbf{L}\cdot\mathbf{S})^2$ terms are given by

$$\mathcal{I}^B_{FF}=2e_{13}l^2(r_{13})(\mathbf{M}\cdot\mathbf{S}\times\mathbf{r}_{12})\cdot Y^p_{12}\ \ (\mathbf{S}\times\mathbf{r}_{12}\cdot\mathbf{M})-2(\boldsymbol{\nabla}F^s_{12}\cdot\mathbf{S}\times\mathbf{r}_{12})\cdot Y^p_{12}(\mathbf{S}\times\mathbf{r}_{12}\cdot\boldsymbol{\nabla}F^s_{12})e_{13}l^2(r_{13})F^{s2}_{13}, \tag{A24}$$

$$\mathcal{I}^B_{FK}=e_{13}\frac{l(r_{13})l'(r_{13})}{r_{13}}((\mathbf{M}\cdot\mathbf{S}\times\mathbf{r}_{12})Y^p_{12}(\mathbf{S}\times\mathbf{r}_{12}\cdot\mathbf{r}_{13})\mathcal{M}+\mathcal{M}(\mathbf{r}_{13}\cdot\mathbf{S}\times\mathbf{r}_{12})Y^p_{12}(\mathbf{S}\times\mathbf{r}_{12}\cdot\mathbf{M}))-\frac{l(r_{13})l'(r_{13})}{r_{13}}$$
$$\times((\boldsymbol{\nabla}F^s_{12}\cdot\mathbf{S}\times\mathbf{r}_{12})Y^p_{12}(\mathbf{S}\times\mathbf{r}_{12}\cdot\mathbf{r}_{13})F^s_{12}-F^s_{12}(\mathbf{r}_{13}\cdot\mathbf{S}\times\mathbf{r}_{12})Y^p_{12}(\mathbf{S}\times\mathbf{r}_{12}\cdot\boldsymbol{\nabla}F^s_{12}))e_{13}F^{s2}_{13}, \tag{A25}$$

$$\mathcal{I}^B_{KK}=\frac{1}{10}e_{13}l^2(r_{13})k_F^2\mathcal{M}(\mathbf{S}\times\mathbf{r}_{12})\cdot Y^p_{12}\ \ (\mathbf{S}\times\mathbf{r}_{12})\ \ \mathcal{M}+\frac{1}{2}e_{13}l'^2(r_{13})[\mathcal{M}\ \ (\mathbf{S}\times\mathbf{r}_{12}\cdot\hat{\mathbf{r}}_{13})Y^p_{12}\ \ (\mathbf{S}\times\mathbf{r}_{12}\cdot\hat{\mathbf{r}}_{13})\ \ \mathcal{M}]$$
$$-F^s_{12}(\mathbf{S}\times\mathbf{r}_{12})\cdot Y^p_{12}\ \ (\mathbf{S}\times\mathbf{r}_{12})F^s_{12}\left(\frac{1}{10}k_F^2l^2(r_{13})-\frac{l'(r_{13})l(r_{13})}{2r_{13}}\right)e_{13}F^{s2}_{13}+\frac{1}{2}F^s_{12}(\mathbf{S}\times\mathbf{r}_{12}\cdot\hat{\mathbf{r}}_{13})Y^p_{12}(\mathbf{S}\times\mathbf{r}_{12}\cdot\hat{\mathbf{r}}_{13})F^s_{12}$$
$$\times\left(l''(r_{13})-\frac{l'(r_{13})}{r_{13}}\right)\times l(r_{13})e_{13}F^{s2}_{13}. \tag{A26}$$

3. Circular exchange diagrams

The two circular exchanges, $e_{23}e_{12}$ and $e_{13}e_{12}$, give identical contributions. We calculate that of $e_{23}e_{12}$ and double the result. In $e_{23}e_{12}$ diagrams, $\Phi^\star\boldsymbol{\nabla}'=\Phi^\star(-i)(\mathbf{k}_3-\mathbf{k}_1)$. The $\mathcal{I}^C$ for L^2 terms are given by

$$\mathcal{I}^C_{FF}=2e_{23}e_{12}l(r_{13})l(r_{23})l(r_{12})(\mathbf{r}_{12}\times\mathbf{M})\cdot(\mathbf{r}_{12}\times\mathbf{M})-2e_2[\mathbf{r}_{12}\times\boldsymbol{\nabla}F^s_{12}]\cdot[\mathbf{r}_{12}\times\boldsymbol{\nabla}F^s_{12}]l(r_{12})l(r_{23})l(r_{13})e_{13}(F^{s2}_{13}-1), \tag{A27}$$

$$\mathcal{I}^C_{FK}=e_{23}e_{12}l(r_{12})l(r_{23})l(r_{31})\left([\mathbf{r}_{12}\times\mathbf{M}]X^p_{12}\cdot[\mathbf{r}_{12}\times\hat{\mathbf{r}}_{32}]\mathcal{M}\frac{l'(r_{23})}{l(r_{23})}+\mathcal{M}[\mathbf{r}_{12}\times\hat{\mathbf{r}}_{13}]X^p_{12}\cdot[\mathbf{r}_{12}\times\mathbf{M}]\frac{l'(r_{13})}{l(r_{13})}\right)$$
$$-e_{12}l(r_{12})l'(r_{23})l(r_{31})([\mathbf{r}_{12}\times\boldsymbol{\nabla}F^s_{12}]X^p_{12}\cdot[\mathbf{r}_{12}\times\hat{\mathbf{r}}_{32}]F^s_{12}+F^s_{12}[\mathbf{r}_{12}\times\hat{\mathbf{r}}_{32}]X^p_{12}\cdot[\mathbf{r}_{12}\times\boldsymbol{\nabla}F^s_{12}])e_{13}(F^{s2}_{13}-1), \tag{A28}$$

$$\mathcal{I}^C_{KK}=e_{23}e_{12}\left(\frac{l'(r_{13})l'(r_{23})l(r_{12})}{2r_{13}r_{23}}(\mathbf{r}_{12}\times\mathbf{r}_{31})\cdot(\mathbf{r}_{12}\times\mathbf{r}_{23})+r_{12}l(r_{13})l(r_{23})l'(r_{12})\right)\times(\mathcal{M}X^p_{12}\mathcal{M})$$
$$-\frac{e_{12}}{2}F^s_{12}X^p_{12}F^s_{12}\left[2r_{12}l'(r_{12})l(r_{23})+r_{12}^2l(r_{12})\times\left(l''(r_{23})[1-(\hat{\mathbf{r}}_{12}\cdot\hat{\mathbf{r}}_{23})^2]+\frac{l'(r_{23})}{r_{23}}[1+(\hat{\mathbf{r}}_{12}\cdot\hat{\mathbf{r}}_{23})^2]\right)\right]l(r_{13})e_{13}(F^{s2}_{13}-1), \tag{A29}$$

while those for the $(\mathbf{L}\cdot\mathbf{S})^2$ terms are given by

$$\mathcal{I}^C_{FF}=2e_{23}e_{12}l(r_{12})l(r_{23})l(r_{13})[\mathbf{M}\cdot\mathbf{S}\times\mathbf{r}_{12}]Y^p_{12}[\mathbf{S}\times\mathbf{r}_{12}\cdot\mathbf{M}]-2e_{12}[\boldsymbol{\nabla}F^s_{12}\cdot\mathbf{S}\times\mathbf{r}_{12}]Y^p_{12}[\mathbf{S}\times\mathbf{r}_{12}\cdot\boldsymbol{\nabla}F^s_{12}]l(r_{12})l(r_{23})l(r_{13})$$
$$\times e_{13}(F^{s2}_{13}-1), \tag{A30}$$

$$\mathcal{I}^C_{FK}=-e_{23}e_{12}\left([\mathbf{M}\cdot\mathbf{S}\times\mathbf{r}_{12}]Y^p_{12}[\mathbf{S}\times\mathbf{r}_{12}\cdot\hat{\mathbf{r}}_{23}]\mathcal{M}\frac{l'(r_{23})}{l(r_{23})}+\mathcal{M}[\hat{\mathbf{r}}_{31}\cdot\mathbf{S}\times\mathbf{r}_{12}]Y^p_{12}[\mathbf{S}\times\mathbf{r}_{12}\cdot\mathbf{M}]\frac{l'(r_{13})}{l(r_{13})}\right)l(r_{12})l(r_{23})l(r_{13})$$
$$+e_{12}([\boldsymbol{\nabla}F^s_{12}\cdot\mathbf{S}\times\mathbf{r}_{12}]Y^p_{12}[\mathbf{S}\times\mathbf{r}_{12}\cdot\hat{\mathbf{r}}_{23}]F^s_{12}+F^s_{12}[\mathbf{S}\times\mathbf{r}_{12}\cdot\hat{\mathbf{r}}_{23}]Y^p_{12}[\mathbf{S}\times\mathbf{r}_{12}\cdot\boldsymbol{\nabla}F^s_{12}])l(r_{12})l'(r_{23})l(r_{13})e_{13}(F^{s2}_{13}-1), \tag{A31}$$

$$\mathcal{I}^C_{KK}=\frac{1}{2}e_{23}e_{12}\mathcal{M}\Big(l(r_{12})l'(r_{23})l'(r_{13})[\mathbf{S}\times\mathbf{r}_{12}\cdot\hat{\mathbf{r}}_{31}]Y^p_{12}[\mathbf{S}\times\mathbf{r}_{12}\cdot\hat{\mathbf{r}}_{23}]+\frac{l'(r_{12})}{r_{12}}l(r_{23})l(r_{13})[\mathbf{S}\times\mathbf{r}_{12}]Y^p_{12}\cdot[\mathbf{S}\times\mathbf{r}_{12}]\Big)\mathcal{M}$$
$$-\frac{1}{2}e_{12}F^s_{12}\Big([\mathbf{S}\times\mathbf{r}_{12}]Y^p_{12}\cdot[\mathbf{S}\times\mathbf{r}_{12}]\Big[\frac{l'(r_{12})}{r_{12}}l(r_{23})l(r_{13})+\frac{l'(r_{23})}{r_{23}}l(r_{12})l(r_{13})\Big]+[\mathbf{S}\times\mathbf{r}_{12}\cdot\hat{\mathbf{r}}_{23}]Y^p_{12}[\mathbf{S}\times\mathbf{r}_{12}\cdot\hat{\mathbf{r}}_{23}]\Big[l''(r_{23})$$
$$-\frac{l'(r_{23})}{r_{23}}\Big]l(r_{12})l(r_{13})\Big)F^s_{12}\times e_{13}(F^{s2}_{13}-1). \tag{A32}$$

APPENDIX B: COMPUTATIONAL METHODS

In Sec. III and Appendix A, the entire 3-body cluster contribution from F^s correlations is expressed as a sum of integrals over $\xi(r_{ij},r_{jk},r_{ki})$, where ξ is a trace of matrices that depend only upon r_{ij},r_{jk}, and r_{ki}. Using spherical symmetry, the integrals over ξ are reduced to 3-dimensional integrals:

$$\int d^3r_{ij}d^3r_{ik}\xi(r_{ij},r_{jk},r_{ki})=8\pi^2\int_0^R dr_{ij}\int_0^{R'}dr_{ik}\int_{|r_{ij}-r_{ik}|}^{r_{ij}+r_{ik}}dr_{jk}\xi(r_{ij},r_{jk},r_{ki}). \tag{B1}$$

The upper limits R and R' are obtained from the range of the interaction and d_t, the range of correlations. We compute this 3-dimensional integral using a grid with $dr\sim 0.1$ fm. The $\mathbf{r}_{ij}$ is chosen as the z-axis and $\mathbf{r}_{ik}$ in the x-z plane to simplify the calculation of v and F matrices.

[1] R.B. Wiringa, S.C. Pieper, J. Carlson, and V.R. Pandharipande, Phys. Rev. C **62**, 014001 (2000).
[2] S.C. Pieper, V.R. Pandharipande, R.B. Wiringa, and J. Carlson, Phys. Rev. C **64**, 014001 (2001).
[3] S.C. Pieper and R.B. Wiringa (private communication).
[4] S.C. Pieper and R.B. Wiringa, Annu. Rev. Nucl. Part. Sci. **51**, 53 (2001).
[5] C.J. Pethick and D.G. Ravenhall, Annu. Rev. Nucl. Part. Sci. **45**, 429 (1995).
[6] H. Heiselberg and V.R. Pandharipande, Annu. Rev. Nucl. Part. Sci. **50**, 481 (2000).
[7] J. Carlson, S. Cowell, J. Morales, D.G. Ravenhall, and V.R. Pandharipande, in Proceedings of the Yukawa International Symposium 01, 2002.
[8] K.E. Schmidt and S. Fantoni, Phys. Lett. B **446**, 99 (1999).
[9] S. Fantoni, A. Sarsa, and K.E. Schmidt, Phys. Rev. Lett. **87**, 181101 (2001).
[10] H.Q. Song, M. Baldo, G. Giansiracusa, and U. Lombardo, Phys. Rev. Lett. **81**, 1584 (1998).
[11] B.D. Day and R.B. Wiringa, Phys. Rev. C **32**, 1057 (1985).
[12] M. Baldo, I. Bombaci, and G.F. Burgio, Astron. Astrophys. **328**, 274 (1997).
[13] R.B. Wiringa, V. Fiks, and A. Fabrocini, Phys. Rev. C **38**, 1010 (1988).
[14] A. Akmal and V.R. Pandharipande, Phys. Rev. C **56**, 2261 (1997).
[15] A. Akmal, V.R. Pandharipande, and D.G. Ravenhall, Phys. Rev. C **58**, 1804 (1998).
[16] S. Fantoni, B.L. Friman, and V.R. Pandharipande, Nucl. Phys. **A399**, 57 (1983).
[17] A. Fabrocini and S. Fantoni, Phys. Lett. B **298**, 263 (1993).
[18] R.B. Wiringa, V.G.J. Stoks, and R. Schiavilla, Phys. Rev. C **51**, 38 (1995).
[19] B.S. Pudliner, V.R. Pandharipande, J. Carlson, S.C. Pieper, and R.B. Wiringa, Phys. Rev. C **56**, 1720 (1997).
[20] V.R. Pandharipande and R.B. Wiringa, Rev. Mod. Phys. **51**, 821 (1979).
[21] I.E. Lagaris and V.R. Pandharipande, Nucl. Phys. **A359**, 349 (1981).
[22] A. Arriaga, V.R. Pandharipande, and R.B. Wiringa, Phys. Rev. C **52**, 2364 (1995).
[23] S. Fantoni and S. Rosati, Nuovo Cimento Soc. Ital. Fis., A **25**, 593 (1975).
[24] J.Z. Zabolitzky, Phys. Rev. A **16**, 1258 (1977).
[25] R.B. Wiringa, Nucl. Phys. **A401**, 86 (1983).
[26] V.R. Pandharipande and H.A. Bethe, Phys. Rev. C **7**, 1312 (1973).
[27] J. Carlson, J. Morales, V.R. Pandharipande, and D.G. Ravenhall (private communication).
[28] H.W. Jackson and E. Feenberg, Ann. Phys. (N.Y.) **15**, 266 (1961).
[29] A. Fabrocini, F. Arias de Saavedra, and G. Co', Phys. Rev. C **61**, 044302 (2000).
[30] S.C. Pieper, R.B. Wiringa, and V.R. Pandharipande, Phys. Rev. C **46**, 1741 (1992).